

## Supporting Information

### **Multi-dimensional construction of a novel active yolk@conductive shell nanofiber web as a self-standing anode for high-performance lithium-ion batteries**

*Hao Liu, Luyi Chen, Yeru Liang, Ruowen Fu, Dingcai Wu\**

*Materials Science Institute, PCFM Lab and GDHPPC Lab, School of Chemistry and Chemical Engineering, Sun Yat-sen University, Guangzhou 510275, P. R. China*

#### **Experimental Section**

*Synthesis of monodisperse modified SiO<sub>2</sub> nanospheres.* SiO<sub>2</sub> nanospheres were synthesized according to Stöber method. In a typical synthesis, two solutions were prepared according to the ratio of ethanol/TEOS = 202.5 ml/22.4 ml, and ethanol/NH<sub>3</sub>·H<sub>2</sub>O/water = 112.5 ml/8.4 ml/104.1 ml, respectively. These two solutions were mixed in a three-necked flask, and then stirred mechanically for 3 h at 30 °C. 2 ml of  $\gamma$ -methacryloxypropyl trimethoxy silane (KH570) dissolved in 100 ml of ethanol was dropped in the three-necked flask for 8 h. Reaction was continued for 36 h. Finally, the modified SiO<sub>2</sub> with particle size of 135 nm was obtained.

*Synthesis of monodisperse SiO<sub>2</sub>@PSDVB nanospheres.* SiO<sub>2</sub>@PSDVB nanoparticles were synthesized according to the ratio of water/styrene/divinyl benzene/sodium dodecyl benzene sulphonate (SDBS)/NaHCO<sub>3</sub>/potassium persulfate (KPS) = 100 ml/4.75 ml/0.25 ml/30 mg/240 mg/120 mg. SDBS and NaHCO<sub>3</sub> were dissolved in deionized water in a four-necked flask at 50 °C. After mechanical stirring for 10 min, 1.2 g of modified SiO<sub>2</sub> ultrasonically dispersed in 10 ml of ethanol was added in the system. Further mechanical stirring for 10 min, styrene and divinyl benzene were added in the system. Temperature was increased to 72 °C

after the system became homogenous with stirring for 10 min, and KPS was added simultaneously. The polymerization was continued for another 12 h. The whole procedure was under the protection of N<sub>2</sub>. The product was washed in toluene via three centrifugation/redispersion cycles and then dried at 70 °C.

*Synthesis of Y<sub>S</sub>S<sub>C</sub>NFW.* In a typical synthesis, 0.1 g of SiO<sub>2</sub>@PSDVB nanospheres and 0.1 g of polyacrylonitrile (PAN) were diluted in 1 ml N,N-dimethylformamide (DMF) under stirring at 60 °C for 4 h to form a homogenous solution. During the electrospinning process, the precursor solution was transported to a metal needle with a flow rate of 1 mL h<sup>-1</sup> by a syringe pump. A flat aluminum foil used as a fiber collector was put about 15 cm away under the needle. A positive direct current (DC) voltage of about 15 kV was applied between the needle and the collector to generate a stable continuous nanofiber that was collected on the foil. Then the electrospun fibers were pre-oxidized in air at 280 °C for 6 h, followed by carbonization for 3 h at 800 °C with a heating rate of 5 °C min<sup>-1</sup> in N<sub>2</sub> flow. The resulting composite was denoted as Y<sub>S</sub>S<sub>C</sub>NFW.

*Structural Characterization.* The morphologies of the samples were investigated by a JSM-6330F scanning electron microscope (SEM) and a JEM-2010HR transmission electron microscope (TEM). The thermogravimetric analysis (TGA) was carried out with a heating rate of 10 °C/min in O<sub>2</sub> flow. XRD pattern was recorded on a D-MAX 2200 VPC diffractometer using Cu Kα radiation (40 kV, 26 mA). The Raman spectrum was obtained with a Renishaw inVia Raman spectrometer. A Micromeritics ASAP 2020 surface area and porosity analyzer was used to analyze the pore structure of the samples. The BET surface area (S<sub>BET</sub>) was determined by Brunauer-Emmett-Teller (BET) theory. The micropore surface area (S<sub>mic</sub>) was determined by t-plot method. The total pore volume (V<sub>t</sub>) was calculated according to the amount adsorbed at a relative pressure P/P<sub>0</sub> of 0.995. The pore size distribution was obtained by original density functional theory (DFT) with non-negative regularization and medium smoothing.

*Electrochemical characterization.* The electrochemical properties were carried out using CR2032 coin-type test cells assembled in an argon-filled glove box with lithium foil as the counter and reference electrodes. The electrochemical measurements were carried out with CR2032 coin-type test cells assembled in an argon-filled glove box. As working electrodes, both the as-prepared self-standing  $Y_5S_6$ CNF and control sample  $SiO_2$ @CNF were directly cut into electrode slices without any current collector, binder or conductive agent. The loading mass was  $0.6 \pm 0.2$  mg  $cm^2$ . The lithium foil was used as the counter and reference electrodes. The discharge-charge measurements were performed at different current densities between the potentials of 0.01-3 V using a Land CT2001A battery test system. Cyclic voltammetry (CV) measurement was carried out at a sweep rate of  $0.1$  mV  $s^{-1}$  with an IM6e electrochemical workstation from 0.01 to 3 V.

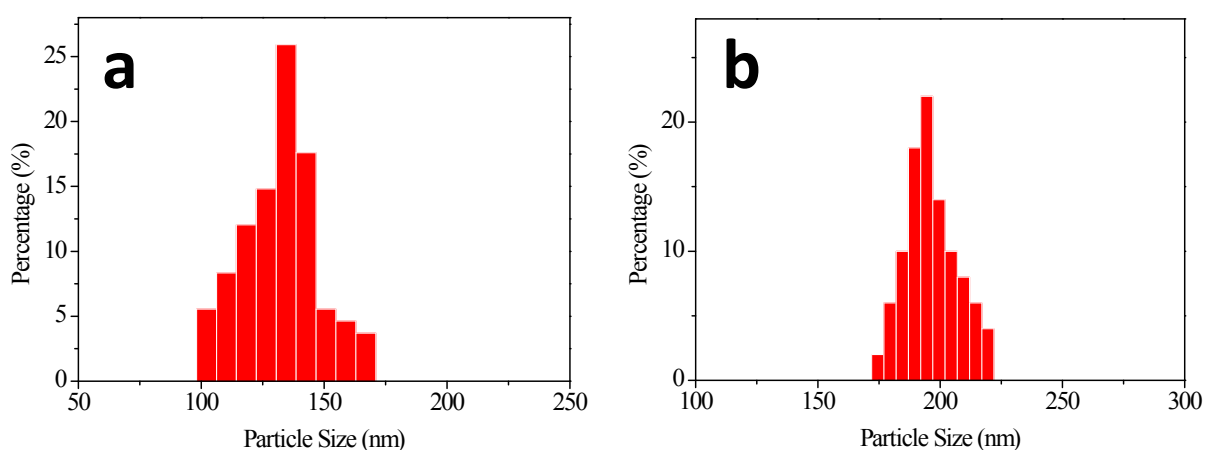


**Fig. S1.** Particle size distribution curves from SEM image analysis for (a)  $SiO_2$  nanospheres and (b)  $SiO_2$ @PSDVB nanospheres.

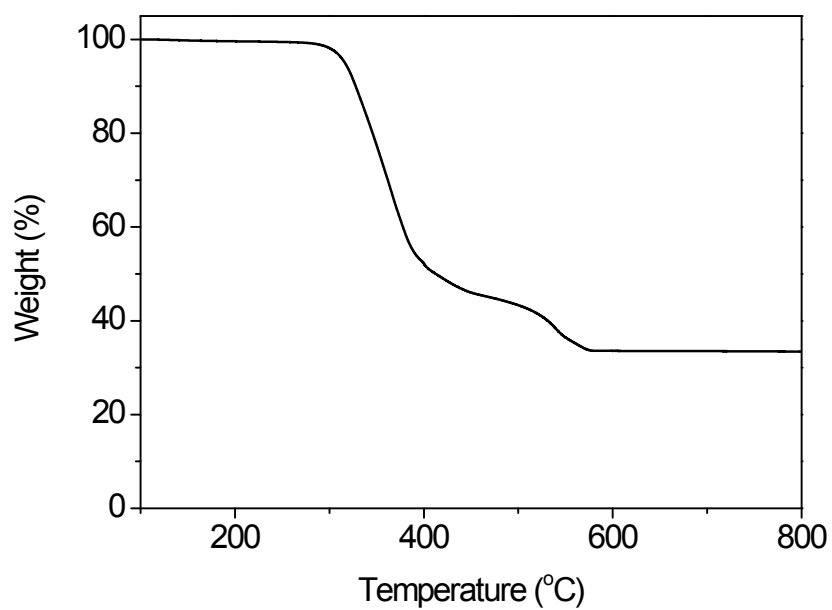


**Fig. S2.** TGA curve of SiO<sub>2</sub>@PSDVB nanospheres.

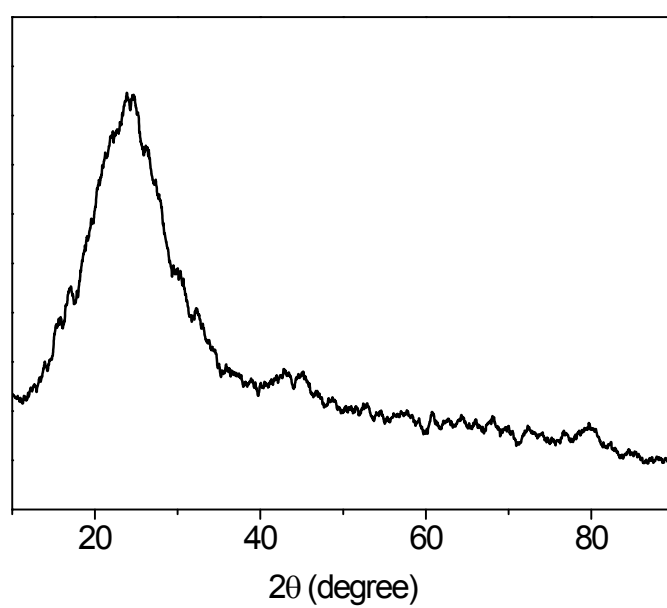


**Fig. S3.** XRD pattern of Y<sub>5</sub>ScNFW. The broad peak around  $2\theta \approx 24^\circ$  demonstrated a graphite-like microcrystalline structure.

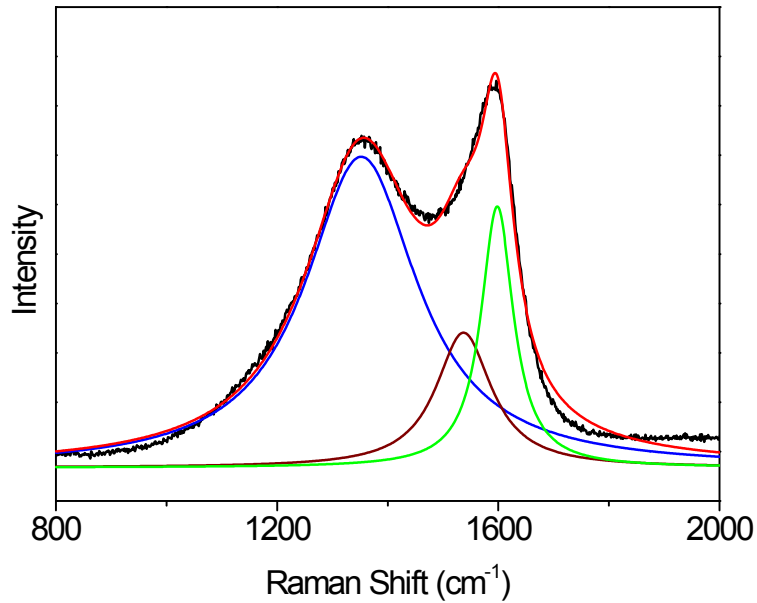


**Fig. S4.** Raman spectrum of  $Y_5S_5C_5NFW$ . This spectrum with a Lorentzian Fit Multipeaks analysis showed that  $Y_5S_5C_5NFW$  presented three bands around 1598, 1537, and 1352  $cm^{-1}$ , indicating a graphite-like microcrystalline structure. The band around 1598  $cm^{-1}$ , denoted as G (graphitic) mode, is associated with “in-plane” zone-center atomic vibrations of large graphite crystallites. The band around 1537  $cm^{-1}$ , regarded as A (amorphous) mode, is related to amorphous  $sp^2$ -bonded forms of carbon arising from interstitial defects of  $Y_5S_5C_5NFW$ . The band around 1352  $cm^{-1}$ , known as D (disordered) mode, is attributed to the phonons near the Brillouin zone boundary active in small crystallites or on the boundaries of larger crystallites. The microcrystalline planar crystal size  $L_a$  for  $Y_5S_5C_5NFW$  can be calculated to be 1.05 nm using the empirical formula found by Tuinstra and Koeing ( $L_a = 4.35I_G/I_D$  (nm), where  $I_G$  and  $I_D$  are the integrated intensities of the G and D modes, respectively).

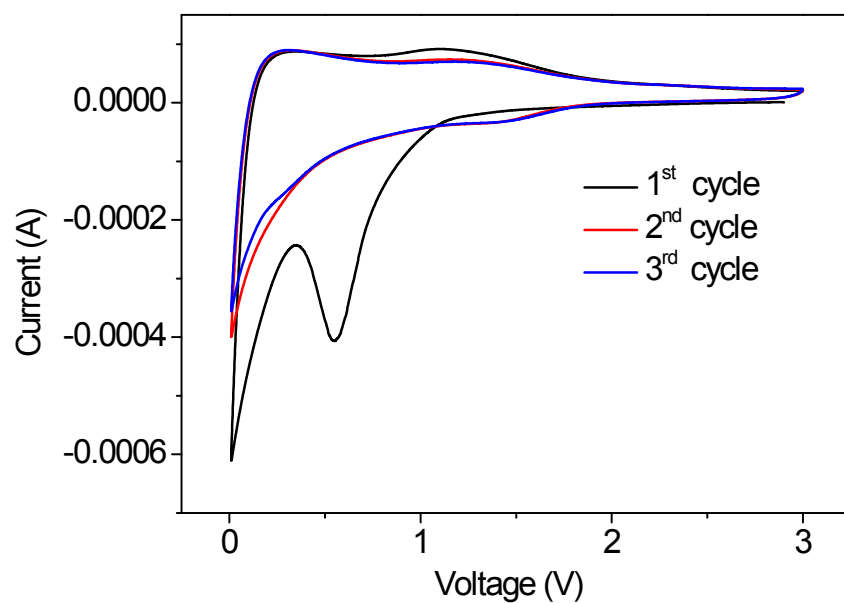


**Fig. S5.** Cyclic voltammograms at a scan rate of  $0.1 \text{ mV s}^{-1}$  between 0.01 V and 3.0 V. All potentials are with reference to  $\text{Li}^+/\text{Li}$ .

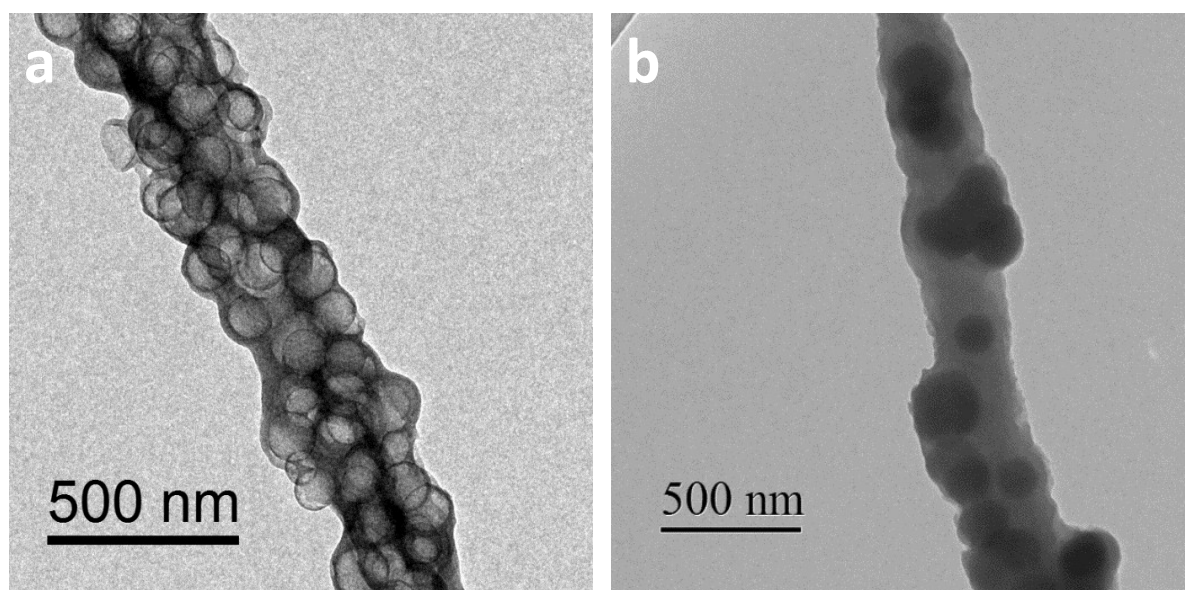


**Fig. S6.** TEM images of (a) HCNF and (b)  $\text{SiO}_2@\text{CNF}$ .

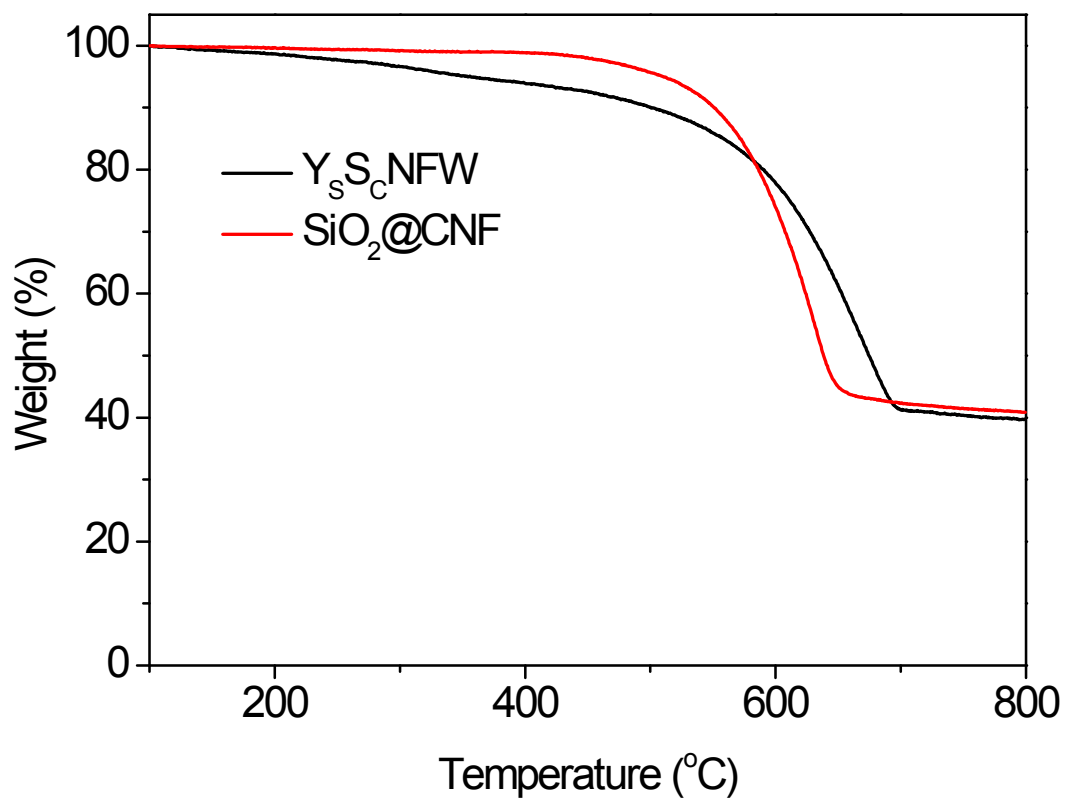


**Fig. S7.** TGA curves of  $Y_5S_5C$ NFW and  $SiO_2@CNF$ .

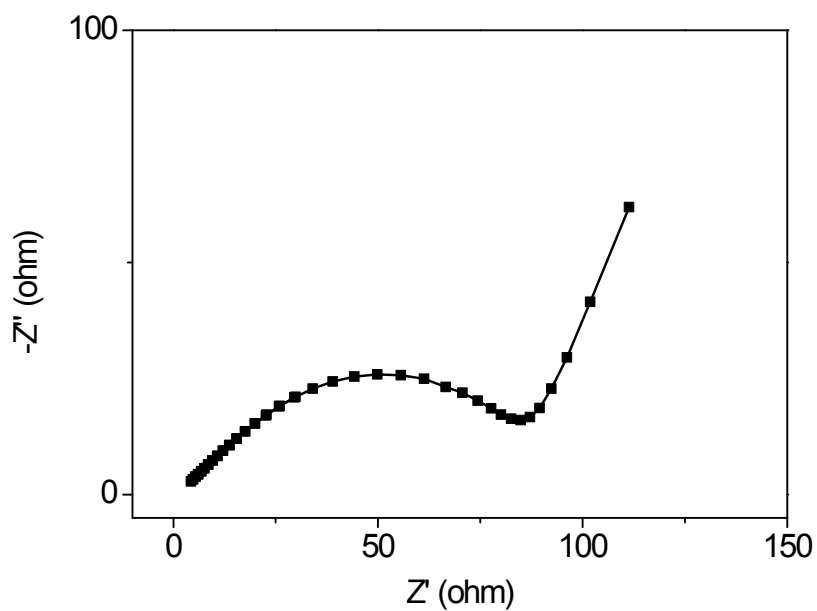


**Fig. S8.** Nyquist plot of  $Y_5S_5C$ NFW. The frequency range for the measurement was 100 kHz-0.1 Hz.

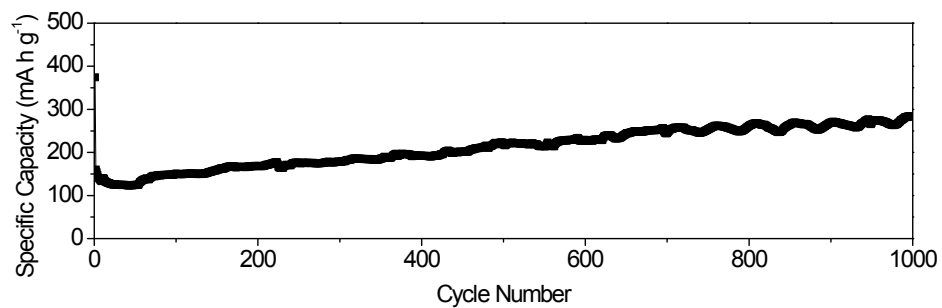


**Fig. S9.** Specific capacity for long-term cycling of Y<sub>5</sub>S<sub>4</sub>C<sub>3</sub>NFW.

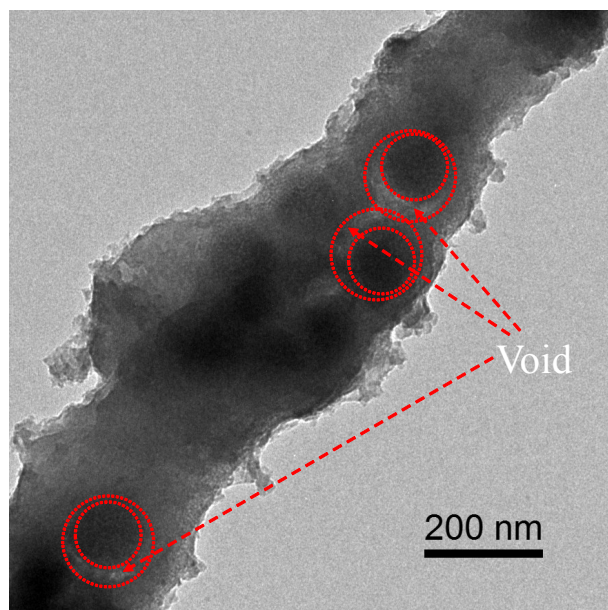


**Fig. S10.** TEM image of Y<sub>5</sub>S<sub>4</sub>C<sub>3</sub>NFW after 1000 discharge/charge cycles as LIB anode.

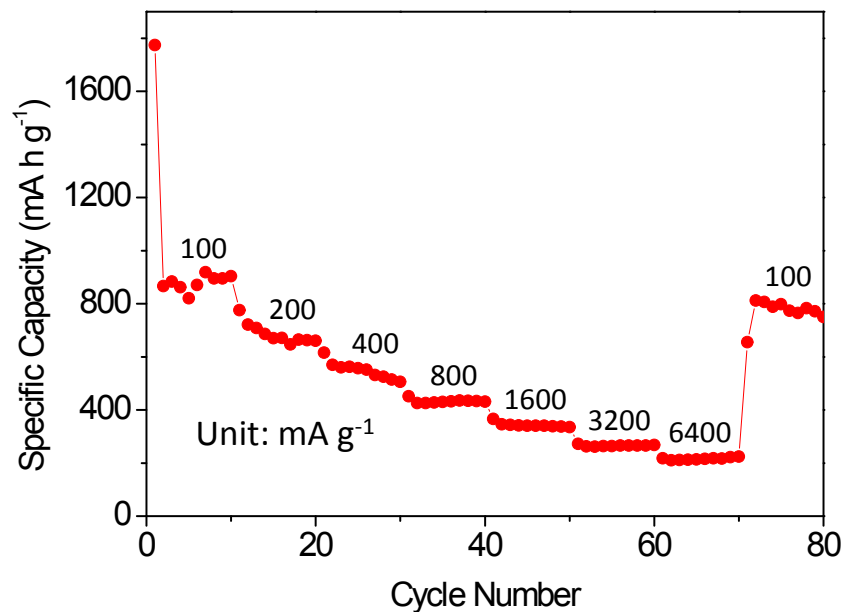


**Fig. S11.** Rate capability of  $Y_5S_5C_5NFW$  at different current densities.

**Table S1** Content of active materials for electrospun nanofiber composites as LIB anodes.

Sample	Content of active materials (wt%)	References
$Y_5S_5C_5NFW$	44.7	This work
SiNP@C	50	1
Si/PAN	16.2	2
PAN/Si	15	3
Porous C/Si composite nanofibers	30	4
Carbon/SnO <sub>2</sub> /carbon core/shell/shell hybrid nanofibers	36	5
Si (core)–hollow carbon nanofiber (sheath) nanocomposite	34.7	6
Si@PCNF	50.2	7

**Table S2** Electrochemical properties of all SiO<sub>2</sub>-based materials and some alternative materials for LIB anodes reported.

Sample	Rate (mA g <sup>-1</sup> )	Specific capacity for composite (mA h g <sup>-1</sup> )	Specific capacity for active components (mA h g <sup>-1</sup> )	References
Y <sub>5</sub> S <sub>C</sub> NFW	100	820, after 130 cycles	1582, after 130 cycles	This work
Milled SiO <sub>2</sub>	100	/	800, after 100 cycles	8
Sn/C composite	450	737, after 200 cycles	/	9
Sn/SnO <sub>2</sub> NCs	1000	700, after 100 cycles	/	10
MnO <sub>x</sub> -C	200	650, after 130 cycles	/	11
N-OMC/SiO <sub>2</sub>	100	740, after 50 cycles	/	12
CS-SG	50	560, after 30 cycles	/	13
SiO <sub>2</sub> NTs	982	/	1266, after 100 cycles	14
SiO <sub>2</sub> @C	75	503, after 103 cycles	/	15
C-SiO <sub>2</sub>	50	500, after 50 cycles	/	16
SiO <sub>2</sub> /C	100	600, after 100 cycles	/	17
Algae derived silica	18	/	500, after 80 cycles	18
RH-900	74	485, after 84 cycles	791, after 84 cycles	19
Carbon@silica	196	351, after 30 cycles	/	20
SiO <sub>2</sub> spheres	1965	/	877, after 500 cycles	21
SiO <sub>2</sub> @C@graphene	50	250, after 200 cycles	/	22

## References

1. T. H. Hwang, Y. M. Lee, B. S. Kong, J. S. Seo, J. W. Choi, *Nano Lett.* **2012**, *12*, 802.
2. L. Ji, K.-H. Jung, A. J. Medford, X. Zhang, *J. Mater. Chem.* **2009**, *19*, 4992.
3. L. Ji, X. Zhang, *Carbon* **2009**, *47*, 3219.
4. L. Ji, X. Zhang, *Electrochem. Commun.* **2009**, *11*, 1146.
5. J. Kong, Z. Liu, Z. Yang, H. R. Tan, S. Xiong, S. Y. Wong, X. Li, X. Lu, *Nanoscale* **2012**, *4*, 525.
6. J. Kong, W. Yee, A. Y. Wei, L. Yang, J. M. Ang, S. L. Phua, S. Y. Wong, R. Zhou, Y. Dong, X. Li, X. Lu, *Nanoscale* **2013**, *5*, 2967.
7. X. Zhou, L. J. Wan, Y. G. Guo, *Small* **2013**, *9*, 2684.
8. W.-S. Chang, C.-M. Park, J.-H. Kim, Y.-U. Kim, G. Jeong, H.-J. Sohn, *Energy Environ. Sci.* **2012**, *5*, 6895.
9. Y. Yu, L. Gu, C. L. Wang, A. Dhanabalan, P. A. Aken, J. Maier, *Angew. Chem. Int. Ed.* **2009**, *48*, 6485.
10. K. Kravchyk, L. Protesescu, M. I. Bodnarchuk, F. Krumeich, M. Yarema, M. Walter, C. Guntlin, M. V. Kovalenko, *J. Am. Chem. Soc.*, **2013**, *135*, 4199.
11. J. C. Guo, Q. Liu, C. S. Wang, M. R. Zachariah, *Adv. Funct. Mater.* **2012**, *22*, 803.
12. Y. R. Liang, L. F. Cai, L. Y. Chen, X. D. Lin, R. W. Fu, M. Q. Zhang, D. C. Wu, *Nanoscale* **2015**, *7*, 3971.
13. X. Q. Yang, H. Huang, Z. H. Li, M. L. Zhong, G. Q. Zhang, D. C. Wu, *Carbon* **2014**, *77*, 275.
14. Z. Favors, W. Wang, H. H. Bay, A. George, M. Ozkan, C. S. Ozkan, *Sci. Rep.* **2014**, *4*, 4605.
15. Y.-K. Kim, J.-W. Moon, J.-G. Lee, Y.-K. Baek, S.-H. Hong, *J. Power Sources* **2014**, *272*, 689.

16. Y. Yao, J. Zhang, L. Xue, T. Huang, A. Yu, *J. Power Sources* **2011**, *196*, 10240.
17. P. Lv, H. Zhao, J. Wang, X. Liu, T. Zhang, Q. Xia, *J. Power Sources* **2013**, *237*, 291.
18. A. Lisowska-Oleksiak, A. P. Nowak, B. Wicikowska, *Rsc Adv.* **2014**, *4*, 40439.
19. L. P. Wang, J. Xue, B. Gao, P. Gao, C. X. Mou, J. Z. Li, *Rsc Adv.* **2014**, *4*, 64744.
20. J. Shu, R. Ma, M. Shui, D. Wang, N. Long, Y. Ren, R. Zhang, J. Yao, X. Mao, W. Zheng, S. Gao, *Rsc Adv.* **2012**, *2*, 5806.
21. J. Tu, Y. Yuan, P. Zhan, H. Jiao, X. Wang, H. Zhu, S. Jiao, *J. Phys. Chem. C* **2014**, *118*, 7357.
22. Y. R. Ren, H. M. Wei, X. B. Huang, J. N. Ding, *Int. J. Electrochem. Sc.* **2014**, *9*, 7784.